

Matrix Integrals and the Counting of Tangles and Links

P. Zinn-Justin

*Department of Physics and Astronomy, Rutgers University,
Piscataway, NJ 08854-8019, USA*

and

J.-B. Zuber

*C.E.A.-Saclay, Service de Physique Théorique,
F-91191 Gif sur Yvette Cedex, France*

Using results on the counting of planar Feynman diagrams derived in matrix models, recent results of Sundberg and Thistlethwaite on the counting of alternating tangles and links are reproduced.

1. Introduction

This is a paper of physical mathematics, which means that it addresses a problem of mathematics using tools of (theoretical) physics. The problem of mathematics is a venerable one, more than a hundred years old, namely the counting of (topologically inequivalent) knots. The physical tools are combinatorial methods developed in the framework of field theory and so-called matrix models. For a review of the history and recent developments of the first subject, see [1]. For an introduction for non physicists to matrix integral techniques, see for example [2–3].

In this note, we show that by combining results obtained recently in knot theory and older ones on matrix integrals, and by using graphical decompositions familiar in field theory, one may reproduce and somewhat simplify the counting of alternating tangles and links performed in [4]. In section 2, we recall basic facts and definitions on knots and their planar projections; we also recall why integrals over large matrices are relevant for the counting of planar objects.

Specifically, we shall consider the following integral

$$\int dM dM^\dagger \exp -N \text{tr} \left(\alpha M M^\dagger - \frac{g}{2} (M M^\dagger)^2 \right). \quad (1.1)$$

over $N \times N$ complex matrices, in the large N limit. In that limit, the integral is represented in terms of *planar* Feynman diagrams, with directed edges and four-valent vertices of the type , which exhibit a close similarity with alternating knot diagrams in planar projection, with crossings represented as . Thus the counting of planar Feynman diagrams (with adequate conditions and weights) must be related to the counting of alternating knots. A substantial part of this paper (section 3) is devoted to eliminating irrelevant or redundant contributions of Feynman diagrams. Once this is achieved, the results of [4] are recovered. In the concluding section, we comment on the possible extensions of these methods.

The observation that planar Feynman diagrams generated by matrix models can be associated to knot diagrams was already made in [5]; the matrix integral proposed there was complicated and had serious convergence problems, so that no explicit calculation was carried out.

2. Basics

2.1. Knots, links and tangles

In this section, we briefly recall some basic concepts of knot theory, referring to the literature for more precise definitions. A *knot* is a smooth circle embedded in \mathbb{R}^3 . A *link* is a collection of intertwined knots (in the following, we shall not consider “unlinks”, i.e. links which can be divided in several non-intertwined pieces). Both kinds of objects are considered up to homeomorphisms of \mathbb{R}^3 . Roughly speaking, a *tangle* is a knotted structure from which four strings emerge: if this object is contained in a ball B with the four endpoints of the strings attached on ∂B , topological equivalence is up to orientation preserving homeomorphisms of B that reduce to the identity on ∂B . The fundamental problem of knot theory is the classification of topologically inequivalent knots, links and tangles.

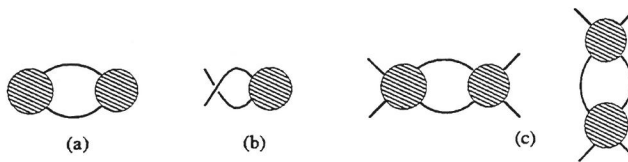


Fig. 1: (a): a non prime link; (b): an irrelevant (or “nugatory”) crossing; (c): 2 particle-reducible tangles, horizontal or vertical sums of two tangles

It is common to represent such objects by their projection in a plane, with under/over-crossings at each double point and with the minimal number of such crossings. To avoid redundancies, we can concentrate on *prime* links and tangles, whose diagrams cannot be decomposed as a sum of components (Fig. 1) and on *reduced* diagrams that contain no irrelevant crossing.

A diagram is called *alternating* if one meets alternatively under- and over-crossings as one travels along each loop. Starting with eight (resp six) crossings, there are knot (resp link) diagrams that cannot be drawn in an alternating way. Although alternate links (and tangles) constitute only a subclass (asymptotically subdominant), they are easier to characterize and thus to enumerate or to count.

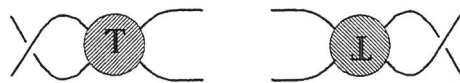


Fig. 2: The flype of a tangle

A major result conjectured by Tait and proved by Menasco and Thistlethwaite [6] is that two alternating reduced knot or link diagrams on the sphere represent the same object if and only if they are related by a sequence of moves acting on tangles called “flypes” (see Fig. 2).

The subproblem that we shall address here is thus the counting of alternating prime links and tangles.

2.2. Matrix Integrals in the large N limit

As a prototype of matrix integrals, we consider the integral over $N \times N$ hermitian matrices

$$Z = \int dM \exp -N \text{tr} \left(\frac{1}{2} M^2 - \frac{g}{4} M^4 \right). \quad (2.1)$$

In order that the integral makes sense, the sign of g should originally be chosen negative. As is well-known, the large N limit allows the analytic continuation to positive values of g . The series expansion of Z in powers of g may be represented diagrammatically by Feynman diagrams, made of undirected edges or “propagators” (2-point functions of the Gaussian model) with double lines expressing the conservation of indices, $\langle M_{ij} M_{k\ell} \rangle_0 = \overbrace{i \longleftarrow \rightarrow l}^j = \frac{1}{N} \delta_{i\ell} \delta_{jk}$, and of four-valent vertices  $= g N \delta_{qi} \delta_{jk} \delta_{\ell m} \delta_{np}$. In the large N limit a counting of powers of N shows that the leading contribution to $\log Z$ is given by a sum of diagrams that may be drawn on the sphere [7], called “planar” by abuse of language. More precisely

$$\lim_{N \rightarrow \infty} \frac{1}{N^2} \log Z = \sum_{\substack{\text{planar diagrams} \\ \text{with } n \text{ vertices}}} \text{weight } g^n \quad (2.2)$$

with a weight equal to one over the order of the automorphism group of the diagram. Once this has been realised, it is simpler to return to a notation with simple lines — and rigid vertices \times . It is this property of matrix integrals to generate (weighted) sums over planar diagrams that we shall use in the context of knot theory.

3. From planar Feynman diagrams to links and tangles

3.1. The matrix integral

As mentionned in the Introduction, in the context of knot theory, it seems natural to consider the integral (1.1) over complex (non hermitian) matrices, in order to distinguish

between under-crossings and over-crossings. However, this integral is closely related to the simpler integral (2.1) in the large N limit. Let us define the partition functions

$$Z^{(1)}(\alpha, g) = \int dM dM^\dagger \exp -N \text{tr} \left(\alpha MM^\dagger - \frac{g}{2} (MM^\dagger)^2 \right) \quad (3.1a)$$

$$Z(\alpha, g) = \int dM \exp -N \text{tr} \left(\frac{1}{2} \alpha M^2 - \frac{g}{4} M^4 \right) \quad (3.1b)$$

and the corresponding “free energies”

$$F^{(1)}(\alpha, g) = \lim_{N \rightarrow \infty} \frac{1}{N^2} \frac{\log Z^{(1)}(\alpha, g)}{\log Z^{(1)}(\alpha, 0)} \quad (3.2a)$$

$$F(\alpha, g) = \lim_{N \rightarrow \infty} \frac{1}{N^2} \frac{\log Z(\alpha, g)}{\log Z(\alpha, 0)} \quad (3.2b)$$

The constant α can be absorbed in a rescaling $M \rightarrow \alpha^{-\frac{1}{2}} M$:

$$Z(\alpha, g) = \alpha^{-\frac{N^2}{2}} Z\left(1, \frac{g}{\alpha^2}\right) \quad (3.3a)$$

$$F(\alpha, g) = F\left(1, \frac{g}{\alpha^2}\right) \quad (3.3b)$$

and similarly for $Z^{(1)}$ and $F^{(1)}$. However, it will be useful for our purposes to keep the parameter α .

The Feynman rules of (3.1a) and those of (3.1b) are quite similar: the former have already been described in Sect. 2.2, while the latter are given by a propagator $\langle M_{ij} M_{k\ell}^\dagger \rangle_0 = \overleftrightarrow{i} \overrightarrow{j} \overleftarrow{k} \overrightarrow{\ell} = \frac{1}{N\alpha} \delta_{i\ell} \delta_{jk}$ and a four-vertex  equal to gN times the usual delta functions. The only difference lies in the orientation of the propagator of the complex theory. However, in the large N “planar” limit, this only results in a factor of 2 in the corresponding free energies, which accounts for the two possible overall orientations that may be given to the lines of each graph of the hermitian theory to transform it into a graph of the non-hermitian one. Therefore

$$F^{(1)}(\alpha, g) = 2F(\alpha, g) \quad (3.4)$$

In addition to the partition functions and free energies, one is also interested in the correlation functions $G_{2n}(\alpha, g) = \langle \frac{1}{N} \text{tr} M^{2n} \rangle$ and $G_{2n}^{(1)}(\alpha, g) = \langle \frac{1}{N} \text{tr} (MM^\dagger)^n \rangle$. The first ones, namely the 2-point and 4-point functions, are simply expressed in terms of F .

$$G_4 = 4 \frac{\partial F}{\partial g} \quad G_4^{(1)} = 2 \frac{\partial F^{(1)}}{\partial g} \quad (3.5)$$

so that $G_4^{(1)} = G_4$ in the large N limit. Furthermore, combining (3.5) with the homogeneity property (3.3), one finds

$$G_2 = \frac{1}{\alpha} - 2 \frac{\partial}{\partial \alpha} F(\alpha, g) = \frac{1}{\alpha}(1 + gG_4) \quad (3.6a)$$

$$G_2^{(1)} = \frac{1}{\alpha}(1 + gG_4^{(1)}) \quad (3.6b)$$

which in particular proves that in the large N limit $G_2 = G_2^{(1)}$.

In that “planar” limit, the function F has been computed by a variety of techniques: saddle point approximation [8], orthogonal polynomials [2], “loop equations” (see [9] for a review). With the current conventions and normalizations,

$$F(\alpha, g) = \frac{1}{2} \ln a^2 - \frac{1}{24}(a^2 - 1)(9 - a^2) \quad (3.7)$$

where a^2 is the solution of

$$3 \frac{g}{\alpha^2} a^4 - a^2 + 1 = 0 \quad (3.8)$$

which is equal to 1 for $g = 0$. We have the expansion

$$\begin{aligned} F(1, g) &= \frac{1}{2} \left(g + \frac{9}{4}g^2 + 9g^3 + \frac{189}{4}g^4 + \dots \right) \\ &= \sum_{p=1}^{\infty} (3g)^p \frac{(2p-1)!}{p!(p+2)!} \end{aligned} \quad (3.9)$$

The 2- and 4-point functions are thus

$$G_2 = G_2^c = \frac{1}{3\alpha} a^2 (4 - a^2) \quad (3.10a)$$

$$G_4 = \frac{1}{\alpha^2} a^4 (3 - a^2) \quad (3.10b)$$

$$G_4^c = G_4 - 2G_2^2 = -\frac{1}{9\alpha^2} a^4 (a^2 - 1)(2a^2 - 5) \quad (3.10c)$$

where G_4^c is the connected 4-point function. More generally, G_{2n} is of the form α^{-n} times a polynomial in a^2 . The singularity of a^2 at $g/\alpha^2 = 1/12$ determines the radius of convergence of F and of the G_{2n} .

3.2. Removal of self-energies

If we want to match Feynman diagrams contributing to the free energy $F^{(1)}$ with *prime* knots or links, we have to eliminate a certain number of redundancies. We have first to eliminate the “self-energy insertions” that correspond either to non prime knots or to irrelevant crossings (“nugatory” in the language of Tait). This is simply achieved by choosing α as a function of g such that

$$G_2(\alpha(g), g) = 1 . \quad (3.11)$$

The function $a^2(g) := a^2(\alpha(g), g)$ is obtained by eliminating α between Eqs. (3.8) and (3.11), i.e.

$$3\frac{g}{\alpha^2}a^4 - a^2 + 1 = 0 \quad (3.8)'$$

$$\frac{1}{3}a^2(4 - a^2) = \alpha \quad (3.11)'$$

which implies that $a^2(g)$ is the solution of

$$27g = (a^2 - 1)(4 - a^2)^2 \quad (3.12)$$

equal to 1 when $g = 0$; $\alpha(g)$ is then given by

$$\alpha(g) = \frac{1}{3}a^2(g)(4 - a^2(g)) . \quad (3.13)$$

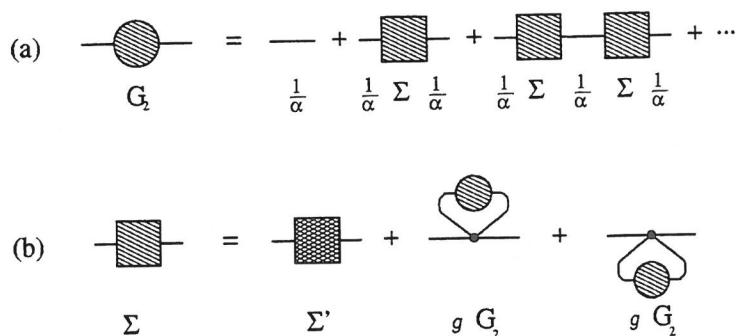


Fig. 3: (a): decomposition of the two-point function into its one-particle-irreducible part; (b) discarding one-vertex-reducible contributions

Let us now consider correlation functions. In field theory, it is common practice to define *truncated* diagrams, whose external lines carry no propagator, and *one-particle-irreducible* ones, that remain connected upon cutting of any line.

The two-point function $G_2(\alpha, g)$ may be expressed in terms of the “self-energy” function Σ

$$G_2(\alpha, g) = \frac{1}{\alpha - \Sigma(\alpha, g)} \quad (3.14)$$

which is the sum of (non-trivial) truncated, one-particle-irreducible graphs (Fig. 3). One can further discard the contributions that are one-vertex-reducible by defining Σ' (see Fig. 3(b))

$$\Sigma'(\alpha, g) = \Sigma(\alpha, g) - 2G_2(\alpha, g) \quad (3.15)$$

If we now remove the self-energy insertions by imposing condition (3.11), we find that Eqs. (3.14) and (3.15) simplify, so that $\Sigma(g) := \Sigma(\alpha(g), g)$ and $\Sigma'(g) := \Sigma'(\alpha(g), g)$ are given by

$$\Sigma(g) = \alpha(g) - 1 \quad (3.16a)$$

$$\Sigma'(g) = \alpha(g) - 1 - 2g \quad (3.16b)$$

i.e. obtained from $\alpha(g)$ by removing the first terms in its expansion in powers of g .

The procedure extends to all correlation functions. Finally one obtains the corresponding “free energy” $F^{(1)}(g)$ by dividing the term of order n of $\Sigma'(g)$ by $2n$ (= number of times of picking a propagator in a diagram of the free energy to open it to a two-point function, cf Eq. (3.6) above).

We may also compute the function $\Gamma(\alpha, g) = G_2^c(\alpha, g)^{-4} G_4^c(\alpha(g), g)$, which counts the truncated (automatically one-particle-irreducible) connected 4-point functions. After removal of the self-energy insertions, $\Gamma(g) := \Gamma(\alpha(g), g)$ becomes simply (Eqs. (3.6a), (3.10c) and (3.16a))

$$\Gamma(g) = \frac{\Sigma'(g)}{g} = 2 \frac{d}{dg} F^{(1)}(g) \quad (3.17)$$

Explicitly,

$$\Gamma(g) = -\frac{1}{(4 - a^2(g))^2} (a^2(g) - 1)(2a^2(g) - 5) \quad (3.18)$$

Perturbatively one finds

$$\begin{aligned}
 a^2(1, g) &= 1 + 3g + 18g^2 + 135g^3 + 1134g^4 + 10206g^5 + 96228g^6 + \dots \\
 G_2(1, g) &= 1 + 2g + 9g^2 + 54g^3 + 378g^4 + 2916g^5 + 24057g^6 + \dots \\
 \alpha(g) &= 1 + 2g + g^2 + 2g^3 + 6g^4 + 22g^5 + 91g^6 + \dots \\
 \Gamma(\alpha(g), g) &= g + 2g^2 + 6g^3 + 22g^4 + 91g^5 + 408g^6 + \dots \\
 F^{(1)}(g) &= \frac{g^2}{4} + \frac{g^3}{3} + \frac{3g^4}{4} + \frac{11g^5}{5} + \frac{91g^6}{12} + \dots
 \end{aligned} \tag{3.19}$$

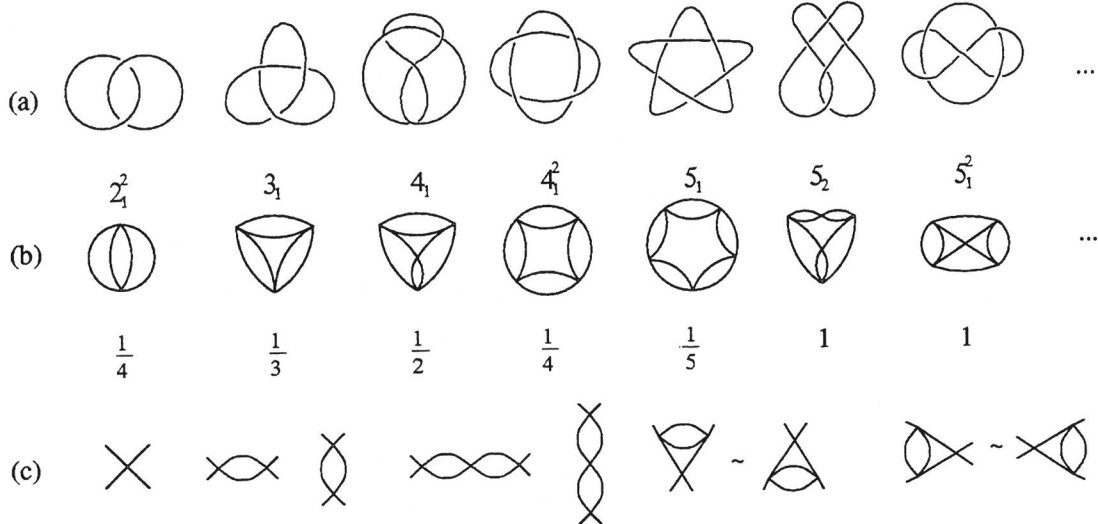


Fig. 4: (a): the first links, with the labelling of [10]; (b) the corresponding diagrams contributing to $F^{(1)}$. For simplicity, the diagrams are not oriented, but the weights are those of the $(MM^\dagger)^2$ theory; (c) diagrams up to order 3 contributing to Γ : the last four are pairwise flype-equivalent.

The first terms of $F^{(1)}$ match the counting of the first prime links weighted by their symmetry factor (see Fig. 4).

$$F^{(1)}(g) = \frac{1}{4}g^2 + \frac{1}{3}g^3 + \left(\frac{1}{2} + \frac{1}{4}\right)g^4 + \left(\frac{1}{5} + 1 + 1\right)g^5 + \dots \tag{3.20}$$

Starting with order 6, however, there is an overcounting of links due to neglecting the flype equivalence. The overcounting occurs already at order 3 if Γ is used to count tangles.

Asymptotic behavior of the coefficients f_n of $F^{(1)}(g)$

The singularity is now given by the closest zero of the equation $g/\alpha^2(g) = 1/12$, which gives $g_* = \frac{4}{27}$. Thus

$$f_n \sim \text{const } b^n n^{-\frac{7}{2}} \tag{3.21}$$

with

$$b = \frac{27}{4} = 6.75 . \tag{3.22}$$

3.3. Two-particle irreducibility

Since the flype acts on tangles, we have to examine more closely the generating function $\Gamma(g)$ of connected 4-point functions with no self-energies. We want to regard the corresponding diagrams as resulting from the dressing of more fundamental objects. This follows a pattern familiar in field theory, whose language we shall follow, while indicating in brackets the corresponding terminology of knot theory.

We say that a 4-leg diagram (a tangle) is *two-particle-irreducible* (2PI) (resp two-particle reducible, 2PR) if cutting any two distinct propagators leaves it connected (resp makes it disconnected). A 2PR diagram is thus the “sum” of smaller components (see Fig. 1). A *fully two-particle-irreducible* diagram is a 4-leg diagram such that any of its 4-leg subdiagrams (including itself) is 2PI. Conversely a fully 2PR diagram (algebraic tangle) is constructed by iterated sums starting from the simple vertex. We shall also make use of *skeletons*, which are generalized diagrams (or “templates”) in which some or all vertices are replaced by blobs (or “slots”). The concepts of fully 2PI skeleton (or basic polyedral template) and of fully 2PR skeleton (algebraic template) follow naturally, with however the extra condition that only blobs should appear in the former.

These blobs may then be substituted by 4-leg diagrams, resulting in a “dressing”. As will appear, the general 4-leg diagram (tangle) results either from the dressing of a fully 2PI skeleton by generic 4-leg diagrams (type I tangles) or from the dressing of non trivial fully 2PR skeletons by type I tangles. The action of flypes will be only on the fully 2PR skeletons appearing in this iteration.

Because in the $(MM^\dagger)^2$ theory with 4-valent vertices, there is no diagram which is two-particle-reducible in both channels, any diagram of $\Gamma(g)$ must be

- i) 2-particle-irreducible in the vertical channel (V-2PI) but possibly 2-particle-reducible in the horizontal one. We denote $V(g)$ the generating function of those diagrams.
- ii) or 2-particle-irreducible in the horizontal channel (H-2PI) but possibly 2-particle-reducible in the vertical one. We denote $H(g)$ the generating function of those diagrams.

Obviously there is some overlap between these two classes, corresponding to diagrams that are 2-particle-irreducible in both channels (2PI), including the simple vertex. Let $D(g)$ denote their generating function. We thus have

$$\Gamma = H + V - D . \quad (3.23)$$

Now since V encompasses diagrams that are 2PI in both channels, plus diagrams that are once 2PR in the horizontal channel (i.e. made of two H-2PI blobs joined by two propagators), plus diagrams twice H-2PR, etc, we have (see Fig. 5)

$$\begin{aligned} V &= D + HH + HHH + \dots \\ &= D + \frac{H^2}{1 - H} . \end{aligned} \quad (3.24)$$

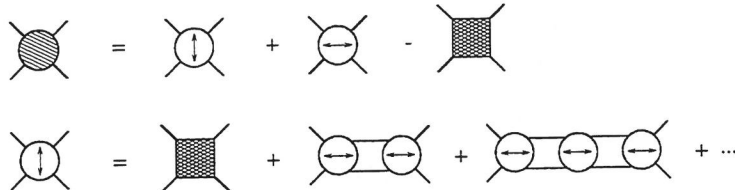


Fig. 5: Graphical representation of Eqs. (3.23) and (3.24).

Since for obvious symmetry reasons, $H = V$, we have the pair of equations

$$\begin{aligned} \Gamma &= 2H - D \\ H &= D + \frac{H^2}{1 - H} . \end{aligned} \quad (3.25)$$

Eliminating H yields

$$D = \Gamma \frac{1 - \Gamma}{1 + \Gamma} . \quad (3.26)$$

Eq. (3.26) can be inverted to allow to reconstruct the function $\Gamma(g)$ out of the 2PI function $D(g)$. For later purposes, we want to distinguish between the single vertex diagram and non-trivial diagrams:

$$D(g) = g + \zeta(g) \quad (3.27)$$

In terms of these new variables, one has:

$$\Gamma(g) = \Gamma\{g, \zeta(g)\} \quad (3.28)$$

(note the braces are used to distinguish the different variables) where

$$\Gamma\{g, \zeta\} = \frac{1}{2} \left[1 - g - \zeta - \sqrt{(1 - g - \zeta)^2 - 4(g + \zeta)} \right] . \quad (3.29)$$

is the generating function

$$\Gamma\{g, \zeta\} = \sum_{m,n} \gamma_{m,n} g^m \zeta^n \quad (3.30)$$

of the number of fully 2PR skeleton diagrams with m vertices and n blobs (algebraic templates, including the trivial one made of a single blob and no vertex). Similarly, one could define $H\{g, \zeta\} = V\{g, \zeta\}$, and of course $D\{g, \zeta\} = g + \zeta$. Note that the function $\Gamma\{g, \zeta\}$ does not depend on the precise form of $\Gamma(g)$, since we have only used the relation (3.26) which was derived from general diagrammatic considerations.

Inversely, we shall need the fully 2PI skeletons which are obtained from $\zeta(g)$ by replacing subgraphs that have four legs with blobs. Defining the inverse function $g[\Gamma]$ of $\Gamma(g)$, the generating function of these skeleton diagrams is simply $\zeta[\Gamma] := \zeta(g[\Gamma])$, or more explicitly

$$\zeta[\Gamma] = \Gamma \frac{1 - \Gamma}{1 + \Gamma} - g[\Gamma]. \quad (3.31)$$

The function $g[\Gamma]$ satisfies by definition $\Gamma(g[\Gamma]) = \Gamma$, and is found by eliminating a^2 between Eqs. (11) and (16). Setting $\eta = 1 - a^2$, we recover the system of [4], [11]:

$$\begin{aligned} 27g &= -\eta(3 + \eta)^2 \\ \Gamma &= -\frac{1}{(3 + \eta)^2} \eta(3 + 2\eta) \end{aligned} \quad (3.32)$$

which leads to

$$g[\Gamma] = \frac{1}{2} \frac{1}{(\Gamma + 2)^3} \left[1 + 10\Gamma - 2\Gamma^2 - (1 - 4\Gamma)^{\frac{3}{2}} \right] \quad (3.33)$$

and finally

$$\zeta[\Gamma] = -\frac{2}{1 + \Gamma} + 2 - \Gamma - g(\Gamma) \quad (3.34)$$

is the desired generating function of fully 2PI skeletons (in the notations of [4], this is $q(g)$). The property mentioned above that Γ is obtained by dressing is expressed by the identity

$$\Gamma(g) = \zeta[\Gamma(g)] + \sum_{\substack{m, n \\ (m, n) \neq (0, 1)}} \gamma_{m, n} g^m \zeta^n [\Gamma(g)] = \Gamma\{g, \zeta(g)\}. \quad (3.35)$$

Perturbatively, we find

$$\begin{aligned} \Gamma(g) &= g + 2g^2 + 6g^3 + 22g^4 + 91g^5 + \dots \\ D(g) &= g + g^5 + 10g^6 + 74g^7 + 492g^8 + \dots \\ \Gamma\{g, \zeta\} &= g + \zeta + 2(g + \zeta)^2 + 6(g + \zeta)^3 + 22(g + \zeta)^4 + 90(g + \zeta)^5 + \dots \\ g[\Gamma] &= \Gamma - 2\Gamma^2 + 2\Gamma^3 - 2\Gamma^4 + \Gamma^5 - 2\Gamma^6 - 2\Gamma^7 - 8\Gamma^8 - 22\Gamma^9 - 68\Gamma^{10} + \dots \\ \zeta[\Gamma] &= \Gamma^5 + 4\Gamma^7 + 6\Gamma^8 + 24\Gamma^9 + 66\Gamma^{10} + \dots \end{aligned} \quad (3.36)$$

The first contributions to $\zeta[\Gamma]$ are depicted on Fig. 6. The closest singularity of $g[\Gamma]$ and of $\zeta[\Gamma]$ is $\Gamma_* = 1/4$ which corresponds to $g[\Gamma_*] = g_* = 4/27$ and $\zeta[\Gamma_*] = 1/540$.

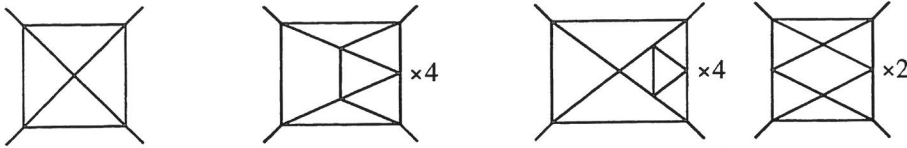


Fig. 6: The first contributions to $\zeta[\Gamma]$. All diagrams can be obtained from the ones depicted by rotations of 90 degrees.

3.4. Quotienting by the flype

The last step is to take into account the flype equivalence; it is borrowed from the discussion of Sundberg and Thistlethwaite and reproduced here for completeness. The fully 2PR skeletons contained in Eq. (3.29) now have to be replaced with skeletons in which the flype equivalence has been quotiented. Then, they have to be dressed by 4-point 2PI functions using Eq. (3.34).

Let $\tilde{\Gamma}\{g, \zeta\}$ be the generating function of the number $\tilde{\gamma}_{mn}$ of *flype-equivalence classes* of fully 2PR skeleton diagrams (algebraic templates) with m vertices and n blobs

$$\tilde{\Gamma}\{g, \zeta\} = \sum_{m,n} \tilde{\gamma}_{m,n} g^m \zeta^n . \quad (3.37)$$

Let $\tilde{H}\{g, \zeta\}$ (resp. $\tilde{V}\{g, \zeta\}$) denote the generating function of flype-equivalence classes of skeletons which are 2PI in the horizontal (resp. vertical) channel, including the single blob and the single vertex. In a way similar to the decomposition performed above for Γ , cf Eq. (3.23), we write

$$\tilde{\Gamma} = \tilde{H} + \tilde{V} - D \quad (3.38)$$

where $D\{g, \zeta\} = g + \zeta$. The equation analogous to Eq. (3.24) is

$$\begin{aligned} \tilde{V} &= D + g\tilde{\Gamma} + (\tilde{H} - g)^2 + (\tilde{H} - g)^3 + \dots \\ &= D + g\tilde{\Gamma} + \frac{(\tilde{H} - g)^2}{1 - (\tilde{H} - g)} \end{aligned} \quad (3.39)$$

where by flyping we can remove the simple vertices inside the \tilde{H} and put them as a single contribution $g\tilde{\Gamma}$.

As before, $\tilde{H} = \tilde{V}$ for symmetry reasons, and after eliminating it one gets an algebraic equation for $\tilde{\Gamma}\{g, \zeta\}$

$$\tilde{\Gamma}^2 - (1 + g - \zeta)\tilde{\Gamma} + \zeta + g \frac{1+g}{1-g} = 0 \quad (3.40)$$

with solution

$$\tilde{\Gamma}\{g, \zeta\} = \frac{1}{2} \left[(1 + g - \zeta) - \sqrt{(1 - g + \zeta)^2 - 8\zeta - 8\frac{g^2}{1-g}} \right], \quad (3.41)$$

which should be compared with Eq. (3.29).

The last step to get the generating function

$$\tilde{\Gamma}(g) := \tilde{\Gamma}\{g, \tilde{\zeta}(g)\} \quad (3.42)$$

of flype equivalence classes of (alternating, prime) tangles is to define $\tilde{\zeta}(g)$ via the relation (3.34), i.e.

$$\tilde{\zeta}(g) = \zeta[\tilde{\Gamma}(g)] \quad (3.43)$$

(The reason we can use Eq. (3.34) without any modification is that fully 2PI skeleton diagrams are not affected by flypes.) In other words, $\tilde{\Gamma}(g)$ is the solution to the implicit equation

$$\tilde{\Gamma}(g) = \tilde{\Gamma}\{g, \zeta[\tilde{\Gamma}(g)]\}, \quad (3.44)$$

where $\zeta[\Gamma]$ and $\tilde{\Gamma}\{g, \zeta\}$ are provided by Eqs. (3.33), (3.34) and (3.41), and which vanishes at $g = 0$.

Perturbatively

$$\tilde{\Gamma}(g) = g + 2g^2 + 4g^3 + 10g^4 + 29g^5 + 98g^6 + 372g^7 + \dots . \quad (3.45)$$

Asymptotic behavior of $\tilde{\Gamma}(g)$: we know the closest singularity of $\zeta[\Gamma]$; we therefore set $\tilde{\Gamma} = \Gamma_* = 1/4$ and $\tilde{\zeta} = \zeta_* = 1/540$ in Eq. (3.40) and solve for g :

$$\tilde{g}_* = \frac{-101 + \sqrt{21001}}{270} . \quad (3.46)$$

This provides the asymptotic behavior of the coefficients \tilde{f}_n of the “free energy” $\tilde{F}^{(1)}(g)$ defined by $\tilde{\Gamma}(g) = 2\frac{d}{dg}\tilde{F}^{(1)}(g)$:

$$\tilde{f}_n \sim \text{const } \tilde{b}^n n^{-\frac{7}{2}} \quad (3.47a)$$

$$\tilde{b} = (101 + \sqrt{21001})/40 \approx 6.147930 . \quad (3.47b)$$

Note that while the first factor \tilde{b}^n in the expansion (“bulk free energy”) is non-universal, the second factor $n^{-7/2}$ is universal (critical behavior of pure gravity [9]; the exponent $\alpha = -\frac{7}{2}$ gives the “string susceptibility” exponent γ of non-critical string theory [12]: $\gamma = \alpha + 3 = -\frac{1}{2}$) and in particular is identical in Eqs. (3.21) and (3.47a). Note also that this free energy counts links with a weight that takes into account the equivalence under flypes and which is less easy to characterize.

4. Concluding remarks

In this paper we have reproduced the results of [4] using prior knowledge of graph counting derived from matrix models, while Sundberg and Thistlethwaite were using results of Tutte [11]. Admittedly the progress is modest. We hope, however, that our method may give some clues on problems that are still open, such as the counting of knots rather than links. To control the number of connected components of a link is in principle easy in our approach. We should consider an integral over n matrices M_α , $\alpha = 1, \dots, n$ interacting through a term $\sum_{\alpha, \beta} (M_\alpha M_\beta^\dagger)^2$ and look at the dependence of $F^{(1)}$ on n . The term linear in n receives contributions only from one-component diagrams, hence after a treatment similar to that of Sect. 3, it should give a generating function of the number of knots, weighted as before by their symmetry factor. Unfortunately, the computation of these matrix integrals and their subsequent treatment (removal of self-energies and flype equivalences) is for generic n beyond our capabilities (see however [13] for a first step in this direction).

Another problem on which matrix technology might prove useful would be in the counting of non alternating diagrams. But there the main problem is knot-theoretic rather than combinatorial: how does one get rid of multiple counting associated with Reidemeister moves?

Acknowledgements

It is a pleasure to acknowledge an informative exchange with V. Jones at the beginning of this work, and interesting discussions with M. Bauer. Part of this work was performed when the authors were participating in the programme on Random Matrices and their Applications at the MSRI, Berkeley. They want to thank Prof. D. Eisenbud for the hospitality of the Institute, and the organizers of the semester, P. Bleher and A. Its, for their invitation that made this collaboration possible. P.Z.-J. is supported in part by the DOE grant DE-FG02-96ER40559.

References

- [1] J. Hoste, M. Thistlethwaite and J. Weeks, *The First 1,701,936 Knots*, *The Mathematical Intelligencer* **20** (1998) 33–48.
- [2] D. Bessis, C. Itzykson and J.-B. Zuber, *Quantum Field Theory Techniques in Graphical Enumeration*, *Adv. Appl. Math.* **1** (1980) 109–157.
- [3] A. Zvonkin, *Matrix Integrals and Map Enumeration: An Accessible Introduction*, *Math. Comp. Modelling* **26** (1997) 281–304.
- [4] C. Sundberg and M. Thistlethwaite, *The rate of Growth of the Number of Prime Alternating Links and Tangles*, *Pac. J. Math.* **182** (1998) 329–358.
- [5] I.Ya. Arefeva and I.V. Volovich, *Knots and Matrix Models*, [hep-th/9706146](#).
- [6] W.W. Menasco and M.B. Thistlethwaite, *The Tait Flyping Conjecture*, *Bull. Amer. Math. Soc.* **25** (1991) 403–412; *The Classification of Alternating Links*, *Ann. Math.* **138** (1993) 113–171.
- [7] G. 't Hooft, *A Planar Diagram Theory for Strong Interactions*, *Nucl. Phys. B* **72** (1974) 461–473.
- [8] E. Brézin, C. Itzykson, G. Parisi and J.-B. Zuber, *Planar Diagrams*, *Commun. Math. Phys.* **59** (1978) 35–51.
- [9] P. Di Francesco, P. Ginsparg and J. Zinn-Justin, *2D Gravity and Random Matrices*, *Phys. Rep.* **254** (1995) 1–133.
- [10] D. Rolfsen, *Knots and Links*, Publish or Perish, Berkeley 1976.
- [11] W.T. Tutte, *A Census of Planar Maps*, *Can. J. Math.* **15** (1963) 249–271.
- [12] V.A. Kazakov and A.A. Migdal, *Recent progress in the theory of non-critical strings*, *Nucl. Phys. B* **311** (1988) 171–190.
- [13] V.A. Kazakov and P. Zinn-Justin, *Two-Matrix Model with ABAB Interaction*, [hep-th/9808043](#), to be published in *Nucl. Phys. B*.